Image Compression using Improved Ridgelet Transform

Mohammed Hussien Miry

Received on : 1/8 /2007
Accepted on :30 / 6 /2008

Abstract

The paper describes approach to the image compression using new hybrid Transforms, namely, the improvement ridgelet transform that has proven to show promising results over ridgelet transform.The hybrid transform based of replacing the wavelet transform with the slantlet transform, the slantlet transform is a discrete wavelet transform with two zero moments and with improved time localization. A comparison was made with compression using ridgelet transform for different images. A high quality image compression has been achieved for natural images. Computer simulation results indicate that the improvement ridgelet transform offers superior and faster compression performance compared to the ridgelet transform based approaches.

Keyword: ridgelet transform, image compression, slantlet transform (SLT).

الخلاصة

في هذا البحث طريقة تقدم لضغط الصور و ذلك باستخدام تحويل مركب جديد يدعى improvement ridgelet transform لتقديم نتائج واعدة افضل . هذا التحويل يعتمد على استبدال تحويل المويجة بتحويل المويل. تحويل المويل هو عبارة عن تحويل المويجة مع العزمين الصفريين و تحسين للزمن المكاني . تمت المقارنة بين تحويل المركب و تحويل المركب المحسن باستخدام صور مختلفة. استرجاع عالي للصورتمثلت للصور الطبيعية. نتائج المحاكاة بالحاسبة اظهرت ان هذا التحويل اعطى نتائج افضل و اسرع من تحويل المركب بعد تطبيقهما على ضغط الصور .

Technology University / Dept. of Electrical and Electronic Engineering, Iraq

1. Introduction

Over the past decade, digital computers, consumer electronics and rapidly evolving telecommunication networks have brought about an information revolution. One of the enabling technologies in facilitating this revolution has been digital data compression[1].

Wavelet based compression of digital signals and images have been a topic of interest for quiet sometime now. In many hundreds of papers published in journals throughout the scientific and engineering disciplines, a wide range of tools and ideas have been proposed and studied. [2]. The degree to which a wavelet basis can yield sparse representation of different signals depends on the time- localization and smoothness property of the basis function. The DWT is usually carried out by filterbank iteration, but for a fixed number of zero moment it does not yield a discrete time basis that is optimal with respect to time-localization. A fundamental trade off exists between time-localization and smoothness characteristics [3]. In this paper, we use The slantlet transform (SLT) as a tool in devising an efficient method for compression of different images.

2. The Discrete Ridgelet Transform

The main idea behind the Ridglet transform is first to apply the two dimensions Discrete Fourier Transform (2-D DFT) to the Two-dimensional signal (image). Next, to map line sampling scheme into a point sampling scheme using the Radon transform. Hence, it is required to take the one dimension inverse Discrete Fourier Transform (1-D IDFT) for each column of the produced two dimensions signal. Finally, it is required to perform the Wavelet transform to each row of the resultant two dimensions signal[4]. Thus the structure of this transform consists of four fundamentals parts, these are:

a) Two dimensions Discrete Fourier Transform (2-D DFT).

b) Radon Transform (RT).

c) One Dimension Inverse Discrete Fourier Transform (1-D IDFT).

d) One Dimension Discrete Wavelet Transform (1-D DWT)

It is expected that this Transform will give a high performance and strong properties. That is because this transform combines together the good properties of the local transforms. The structure of the Discrete Ridgelet Transform is given in Figure.1.

2.1 Radon Transform

The order of the coefficients in the corresponding Fourier slices are controlled by the direction of a set of normal vectors, namely, (a_k,b_k), where k=0,1,2,....*p*.

It was shown that the optimum number of radon projections is *p+1*, one projection for each column, and the best ordering of the 2DFFT coefficients in these projections which is controlled by the normal

vectors can be achieved if the normal vectors determined from:

$$(a_k, b_k) = \arg \min_{\substack{(a_k,b_k)\in\{nu_k:1\le n\le p\} \\ nu.C_p(b_k)\ge 0}} \left\| (C_p(a_k), C_p(b_k)) \right\| \quad \ldots (1)$$

Here $C_p(x)$ denotes the centralized function of period *p*; $Cp(x) = x\text{-}p.round(x/p)$. Hence, $\left\| (C_p(a_k), C_p(b_k)) \right\|$ represents the distance from the origin to the point (a_k,b_k) on the Fourier plane. The constraint $Cp(b_k) \geq 0$ is imposed in order to remove the ambiguity in deciding between (a,b) and $(-a,-b)$ as the normal vector for the projection. As a result the optimal normal vectors are restricted to have angles in $(0,\pi)$. Now, the matrix *F* is assigned the symbol $F_{opt.}$, after the reordering[5].

2.2 Improved Ridgelet Algorithm

The main idea of this improvement is to replace the Wavelet Transform in the Ridgelet Transform structure by the Slantlet Transform. Since the Slantlet Transform is an orthogonal DWT and provides improved

time localization than the DWT [3]. So that this new Hybrid Transform will give a high performance and strong properties.

2.3 Slantlet Transform

The SLT uses a special case of a class of bases described by Alpert [6], the construction of which relies on Gram–Schmidt orthogonalization. The SLT is based on a filterbank structure where different filters are used for each scale. Let us consider a usual two-scale iterated DWT filterbank shown in Fig. 2 and its equivalent form Fig. 3 The SLT filterbank employs the structure of the equivalent form shown in Fig. 3 ,but it is occupied by different filters that are not products. With this extra degree of freedom obtained by giving up the product form, filters of shorter length are designed satisfying orthogonality and zero moment conditions. For two-channel case the Daubechies filter [7] is the shortest filter which makes the filterbank orthogonal and has K zero moments. For K zero moments the iterated filters of Fig. 3(a, b) are of lengths 10 and 4 but the SLT filterbank with K=2 zero moments shown in Fig. 3(a, b) has filter lengths 8 and 4. Thus the two-scale SLT filterbank has a filter length which is two samples less than that of a two-scale iterated Daubechies-2 filterbank. This difference grows with the number of stages. Some characteristic features of the SLT filterbank are orthogonal, having two zero moments and has octave-band characteristic. Each filterbank has a scale dilation factor of two and provides a multiresolution decomposition. The slantlet filters are piecewise linear. [8]. We will denote, by scale i , the scale with which $g_i(n)$,$f_i(n)$, and $h_i(n)$ analyze a signal. The length of the filters for scale i will be proportional to 2^i. That is approximately true for iterated filterbanks; however, it is exact for slantlet filterbanks. In general, the support of $g_i(n)$,$f_i(n)$, and $h_i(n)$ will be 2^{i+1} . We should clarify the way in which the slantlet filterbanks in Fig.3 are generalized to ℓ scales. This is done as follows: The ℓ-scale filterbank has 2ℓ channels. The low pass filter is to be called $h_i(n)$. The filter adjacent to the low pass channel is to be called $f_i(n)$. Both $h_i(n)$ and $f_i(n)$ are to be followed by downsampling by 2^{ℓ}. The remaining 2ℓ-2 channels are filtered by $g_i(n)$ and its shifted time-reverse for subscale i=1,..., ℓ-1 . Each is to be followed by downsampling by 2^{i+1} . It follows that the filterbank is critically sampled. Note that in the slantlet filterbank, each filter $g_i(n)$ appears together with its time reverse. While $h_i(n)$ does not appear with its time reverse, it always appears paired with the filter $f_i(n)$. In addition, note that the ℓ-scale and ℓ+1–scale filterbanks have in common the filters for and their time-reversed versions[8].

2.3.1 Derivations of Filters

Because the sought-after filter $g_i(n)$ is to be linear over the two above-mentioned intervals, it is described by four parameters and can be written as

$$g(n)=\begin{cases} a_{0,0}+a_{0,1}n, \; for.n=0..2^{i}-1 \\ a_{1,0}+a_{1,1}(n-2^{i}), \; for.n=2^{i},..2^{i+1}-1 \end{cases} \quad (2)$$

Where

$$a_{0,0} = (s_0 + t_0)/2$$

$$a_{1,0} = (s_0 - t_0)/2$$

$$a_{0,1} = (s_1 + t_1)/2$$

$$a_{1,1} = (s_1 - t_1)/2$$

$$s_0 = -s_1.(m-1)/2$$

$$t_0 = ((m+1)s_1/3 - m t_1)(m-1)/2m$$

$$s_1 = 6\sqrt{m/((m^2-1)(4m^2-1))}$$

$$t_1 = 2\sqrt{3/(m.(m^2-1))}$$

$$m = 2^i$$

Therefore, to obtain such that the sought-after –scale filterbank is orthogonal with two zero moments requires obtaining

parameters and so that we have the following.

1)$g_i(n)$ is of unit norm for each scale i.

$$\sum_{n=0}^{2^{i+1}-1} g_i^2(n) = 1 \quad (3)$$

2) $g_i(n)$ is orthogonal to its shifted time reverse.

$$\sum_{n=0}^{2^{i+1}-1} g_i(n) g_i(2^{i+1}-1-n) = 0 \quad (4)$$

$$\sum_{n=0}^{2^{i+1}-1} g_i(n) = 0 \quad (5)$$

$$\sum_{n=0}^{2^{i+1}-1} n g_i(n) = 0 \quad (6)$$

Each of the conditions can be written as an algebraic equation in terms of the four parameters $a_{0,0}$,$a_{0,1}$,$a_{1,0}$ and $a_{1,1}$.

Note that the parameters $a_{0,0}$,$a_{0,1}$,$a_{1,0}$ and $a_{1,1}$ depend on i The same approach works for $f_i(n)$ and $h_i(n)$. Using, again, a piecewise linear form $f_i(n)$ and $h_i(n)$ can be written in terms of eight unknown parameters $b_{0,0}$,$b_{0,1}$,$b_{1,0}$ $b_{1,1}$, $c_{0,0}$,$c_{0,1}$,$c_{1,0}$ and $c_{1,1}$

$$h_i(n) = \begin{cases} b_{0,0} + b_{0,1} n, & for \quad n = 0,\ldots 2^i - 1 \\ b_{1,0} + b_{1,1}(n - 2^i), & for \quad n = 2^i,\ldots,2^{i+1} - 1 \end{cases} \quad (7)$$

$$f_i(n) = \begin{cases} c_{0,0} + c_{0,1} n, & for\ n=0,..2^i - 1 \\ c_{1,0} + c_{1,1}(n - 2^i), & for\ n=2^i,\ldots 2^{i+1} - 1 \end{cases} \quad (8)$$

Where

$b_{0,0} = u.(v+1)/(2m)$

$b_{1,0} = u - b_{0,0}$

$b_{0,1} = u/m$

$b_{1,1} = -b_{0,1}$

$q = \sqrt{3/(m.(m^2-1))/m}$

$c_{0,1} = q.(v - m)$

$c_{1,1} =$ n

$c_{1,0} =$ +1−2m)/2

$c_{0,0} = c_{0,1}.(v+1)/2$

$u = 1/\sqrt{m}$

$v = \sqrt{(2m^2+1)/3}$

$m = 2^i$

The orthogonality and moment conditions require the following.

1) $f_i(n)$ and $h_i(n)$ are of unit norm for scale i. (5)

$$\sum_{n=0}^{2^{i+1}-1} h_i^2(n) = 1 \quad (9)$$

$$\sum_{n=0}^{2^{i+1}-1} f_i^2(n) = 1 \quad (10)$$

2) $f_i(n)$ and $h_i(n)$ are orthogonal to their shifted versions.

$$\sum_{n=0}^{2^i-1} h_i(n) h_i(n+2^i) = 0 \quad (11)$$

$$\sum_{n=0}^{2^i-1} f_i(n) f_i(n+2^i) = 0 \quad (12)$$

$$\sum_{n=0}^{2^{i+1}-1} h_i(n) f_i(n) = 0 \quad (13)$$

$$\sum_{n=0}^{2^i-1} h_i(n) f_i(n+2^i) = 0 \quad (14)$$

3) $f_i(n)$ annihilates linear discrete polynomials. (8)

$$\sum_{n=0}^{2^{i+1}-1} f_i(n) = 0 \quad (15)$$

$$\sum_{n=0}^{2^{i+1}-1} n f_i(n) = 0 \quad (16)$$

We make several comments regarding Fig. 3

.

1) Each filterbank (equivalently, discrete-time basis) is orthogonal with itself. The

filters in the synthesis filterbank are obtained by time reversal of the analysis filters.
2) Each filterbank has two zero moments. The filters (except for the low pass ones) annihilate discrete-time polynomials of degree less than 2. Because it represents equation of line.
3) Each filterbank has an octave-band characteristic.
4) The scale-dilation factor is 2 for each filterbank. Between scales, the filters dilate by roughly a factor of 2. (In the slantlet filterbanks, they dilate by exactly a factor of 2.)
5) Each filterbank provides a multiresolution decomposition. By discarding the high pass channels and passing only the low pass channel outputs through the synthesis filterbank, a lower resolution version of the original signal is obtained.
6) The slantlet filterbank is less frequency selective than the traditional DWT filterbank due to the shorter length of the filters. The time localization is improved with a degradation of frequency selectivity.
7) The slantlet filters are piecewise linear [8].

We note that $h_i(n)$ and $f_i(n)$ specialize to the Daubechies length-4 filters for i=1 , as expected. Fig .5 show slantlet transform for the image in the Fig.4 .

2.3.2 Filters Length

In Fig.3 , it was seen that the support of the slantlet filters is less than those of the filters obtained by filterbank iteration. It is interesting to note the difference for the general ℓ-scale case. The iterated filterbank, with Daubechies length-4 filters, analyzes scale with a filter of length $3*2^i-2$. On the other hand, the slantlet filterbank analyzes scale with the filter $g_i(n)$ of length 2^{i+1} . That gives a reduction of 2^i-2 samples for scale i. The ratio tends to two thirds as i increase (for coarser scales). That reduction in the support of the analysis filters is precisely what was sought[8].

3. Proposed Improve Ridgelet Transform Based Image Compression

The main block diagram of the image compression using Improve Ridgelet Transform consists of two stages, namely the Image Encoder(compression stage) and the Image decoder(decompression stage). Fig.6 shows compression encoder.

3.1 Compression Steps

The following steps are followed in the encoder phase:
We taking Improve Ridgelet Transform for an input image. In this step the image decompose to Ridgelet coefficients. In certain signals, many of the Ridgelet coefficients are close or equal to zero. Through a method called thresholding, these coefficients may be modified so that the sequence of slantlet coefficients contains long strings of zeros.The final step of the process, known as quantization, converts a sequence of floating numbers to a sequence of integers. The simplest form is to round to the nearest integer.

3.2 Decompression Steps

The stages of image Decoder are shown in Fig .7. To get the reconstructed image, we apply the inverse improve ridgelet transform on compressed image.

4. Simulation Result

Following the study of the efficiency of the improved ridgelet transform, we perform a numerical comparison on the gray image (3 images) of the same function using two competitive transforms: improved ridgelet transform and ridgelet transform. Table 1 show the difference between the : improved ridgelet transform and ridgelet transform. we note that the length of filter of the slantlet transform is smaller than wavelet filters and equation of it is linear, for this reason the improved ridgelet transform achieves the best performance, as expected from the continuous theory.

5. Conclusion

In this paper, we presented a strategy for newly build ridgelet transform for gray-

scaled image compression. The resulting implementation is found to posses high reconstruction property and provides better compression ratios as compared to ridgelet transform. The measure criterion for comparison was PSNR, which can be calculated directly from the original and reconstructed data.
The relation of peak signal to noise ratio, defined it as shown in Eq. (17) below:

$$SNR_{PEAK} = 10 \log \left(\frac{(255)^2}{\frac{1}{N} \sum_{r=0}^{N-1} \sum_{c=0}^{N-1} \left[\hat{I}(r,c) - I(r,c) \right]^2} \right) \quad (17)$$

The comparison of ridgelet transform and the proposed ridgelet transform codec for the test image . In terms of statistical error, proposed ridgelet transform codec gives higher signal to noise ratio in three of the examples

In this paper, the : improved ridgelet transform has been applied for compression of image. The compression performance of the new approach is assessed through computer simulation and the results are compared with the DWT approaches, it is, in general, observed that the accuracy of the reconstruction of the proposed SLT method is better than that DWT. Exhaustive computer simulation results on different image signals indicate this trend. Thus it is, in general, concluded that the SLT based compression technique yields better performance compared to the DWT.

Reference

1- P. Stan., "**Implementation and Analysis of Eidochromatic Transform for Color Image Compression** ",May, 2005 .

2- A. Mansoor and A. B. Mansoor,"**The Curvelet Transform for Digital Image Compression**",E-mail: awais.mansoor@gmail.com,atif@zararshaeedtrust.org.

3- G. Panda, P. K. Dash, A. K. Pradhan, and S. K. Meher, "**Data Compression of Power Quality Events Using the Slantlet Transform** ",IEEE Trans . Power Delivery, vol. 17, no. 2, April 2002.

4- M. N. Donoho," **Finite Ridgelet Transform for Image represenration**" IEEE Trans. Image Processing Ip EDICS:2-WAVP April 2001.

5- O. M.. Faraj and W. Al-Jawhar, " **Design and Simulation of a Proposed Radon Based OFDM Transceiver** ", IPEC-30; The 6th International Philadelphia Engineering Conference On IPEC2006, Jordan.

6- A.Alpert,"**A class of bases in l2 for the sparse representation of integral operators**", SIAM J. Math. Anal., vol. 24, no. 1, pp. 246–262, Jan. 1993. 7- I. Daubechies," **Ten Lectures on Wavelets**", Philadelphia, PA: SIAM,1992.

8- I. W. Selesnick, "**The slantlet transform,**" IEEE Trans. Signal Processing,vol. 47, pp. 1304–1313, May 1999.

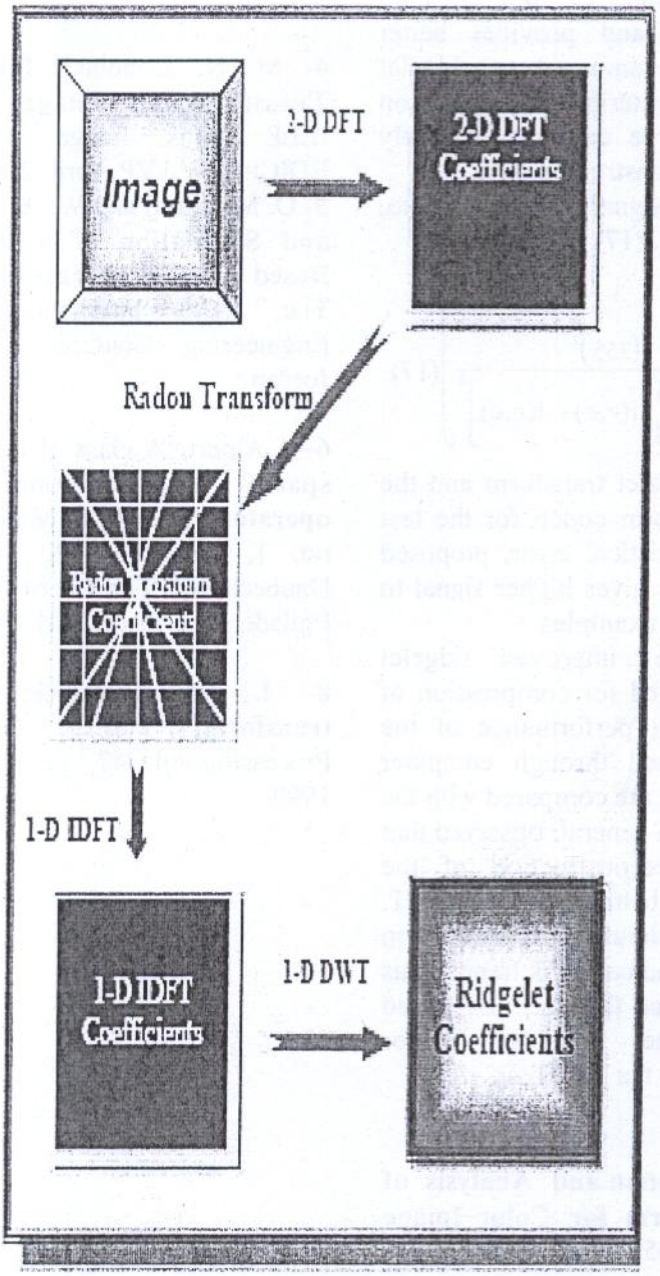

Figure .1 Block diagram of ridgelet transform

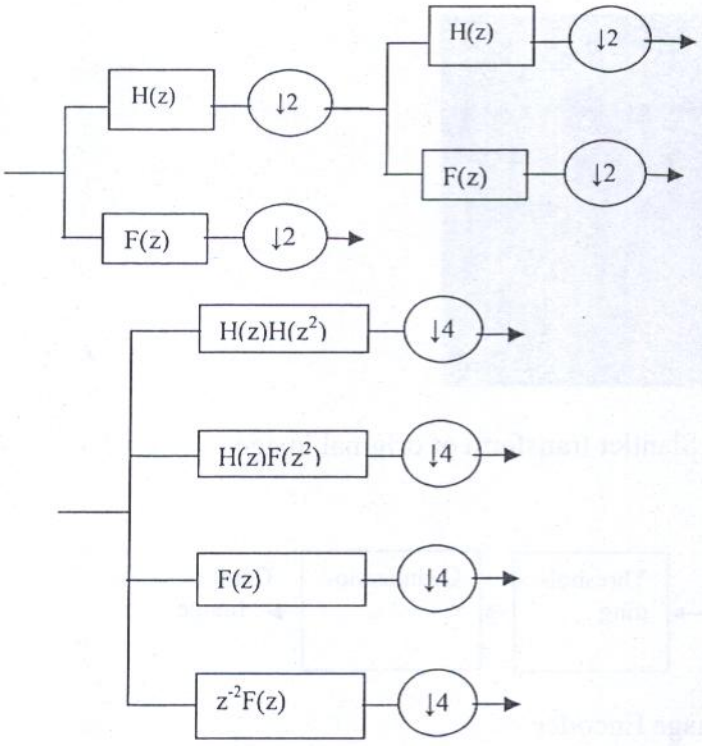

Figure .2. a Two-scale Filterbank
b An Equivalent

Figure. 4 Original image

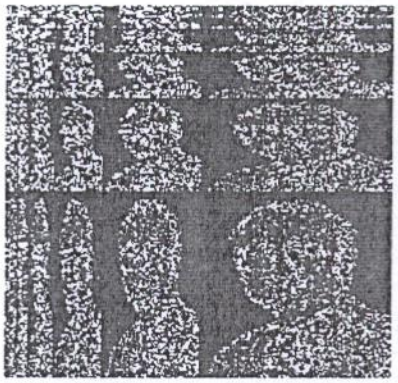

Figure. 5 Slantlet transform of original image

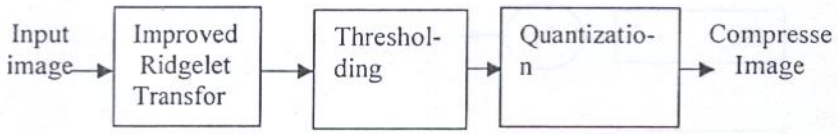

Figure .6 Image Encoder

Figure .7 Image Decoder

Table 1
compression ratio and the PSNR in dB obtained using the improve ridgelet transform and ridgelet transform based compression for different image .

Image	Transform	CR 92%	CR 95%	CR 97%
1	Improve Ridgelet	27.42 dB	26.64 dB	25.46 dB
	Ridgelet	26.77 dB	25.70 dB	23.52 dB
2	Improve Ridgelet	25.58 dB	24.76 dB	23.44 dB
	Ridgelet	24.82 dB	23.64 dB	21.11 dB
3	Improve Ridgelet	29.83 dB	28.93 dB	27.32 dB
	Ridgelet	29.13 dB	27.87 dB	24.94 dB